

Magnetic structure of CuCrO_2 : a single crystal neutron diffraction study

M. Frontzek¹, G. Ehlers¹, A. Podlesnyak¹, H. Cao¹, M. Matsuda¹, O. Zaharko², N. Aliouane², S. Barilo³, S.V. Shiryayev³

¹Neutron Scattering Science Division, Oak Ridge National Laboratory, Oak Ridge, TN 37831, USA

²Laboratory for Neutron Scattering, Paul Scherrer Institute, CH-5232 Villigen, Switzerland

³Institute of Solid State and Semiconductor Physics, Minsk 220 072, Belarus

E-mail: frontzekmd@ornl.gov

Abstract. This paper presents results of a recent study of multiferroic CuCrO_2 by means of single crystal neutron diffraction. This system has two close magnetic phase transitions at $T_{\text{N}1} = 24.2$ K and $T_{\text{N}2} = 23.6$ K. The low temperature magnetic structure below $T_{\text{N}2}$ is unambiguously determined to be a fully 3-dimensional proper screw. Between $T_{\text{N}1}$ and $T_{\text{N}2}$ antiferromagnetic order is found that is essentially 2-dimensional. In this narrow temperature range, magnetic near neighbor correlations are still long range in the (H, K) plane, whereas nearest neighbors along the L -direction are uncorrelated. Thus, the multiferroic state is realized only in the low-temperature 3-dimensional state and not in the 2-dimensional state.

PACS numbers: 75.25+z, 75.47.Lx, 75.85.+t

1. Introduction

Multiferroic materials have become of interest for their unusual low-temperature properties in general, and in particular for the observation that one can affect their magnetic structure through an electric field and their electric polarization through a magnetic field. The most promising candidates for a controllable multiferroic have been found among the materials with inherent geometric magnetic frustration [1].

The magnetic properties of the delafossite CuCrO_2 have received detailed interest since the discovery of its multiferroic behaviour [2–4]. This system, which crystallizes in the rhombohedral $R\bar{3}m$ space group, is a multiferroic compound due to its apparent strong coupling of spin and charge. In contrast to other multiferroic compounds CuCrO_2 shows a spontaneous electric polarization upon antiferromagnetic ordering without an accompanying structural phase transition, although a slight in-plane lattice distortion can be measured [5]. Further, CuCrO_2 is a rare example of a system whose magnetoelectric properties are tunable by both an electric and a magnetic field [3, 6]. Another particular property is that the multiferroic state is already entered in zero magnetic field as opposed to isostructural CuFeO_2 [7–9].

Several studies of the magnetic structure by neutron diffraction techniques with powder [10, 11] and single crystal [6, 12] samples have been reported. The powder experiments found an incommensurate magnetic propagation vector $\boldsymbol{\tau} = (0.329, 0.329, 0)$ based on the position of the $(0, 0, 0) + \boldsymbol{\tau}$ reflection, and a broadening of some of the magnetic Bragg peaks which was attributed to short range correlations along the L -direction, either in the form of quasi 2-dimensionality [10] or stacking faults [11]. The measured powder intensities were best described with a proper-screw magnetic structure, although other magnetic structure models could not be unambiguously excluded. The single crystal experiments, on the other hand, identified the structure as an incommensurate proper screw but the magnetic moments were not refined, and, most importantly, measurements were only reported for $(H, K, 0)$ reflections [6, 12]. Thus the question of possible ordering along the L -direction was not considered. In this contribution we will fill these gaps and arrive at the following main conclusions. The low-temperature magnetic structure below $T_{\text{N}2}^\ddagger$ is truly 3-dimensional with long range correlations along the L -direction. We confirm the incommensurate proper screw magnetic spiral propagating along the $[1, 1, 0]$ direction, and find that it has an elliptical envelope with a modulation between $\mathbf{M}_{[1\bar{1}0]} = 2.2(2) \mu_{\text{B}}$ and $\mathbf{M}_{[001]} = 2.8(2) \mu_{\text{B}}$. Furthermore we characterize the spin structure in the intermediate temperature phase between $T_{\text{N}1}$ and $T_{\text{N}2}$ (which is not multiferroic) as 2-dimensional with a total lack of near neighbor magnetic correlations along the L -direction.

‡ opposite from [3] we define $T_{\text{N}2} < T_{\text{N}1}$

2. Experimental

Single crystal samples were prepared in two ways. Samples up to 6 mm^3 in size were grown in a platinum crucible from the high temperature solution technique based on the thermal decomposition of $\text{K}_2\text{Cr}_2\text{O}_7$ at 860°C in the presence of CuO [13]. The mixture of $\text{K}_2\text{Cr}_2\text{O}_7$ (73 mol%) and CuO (27 mol%) was placed into a high density aluminum crucible and heated quickly up to 850°C . Then the temperature was lowered at a rate of 0.5°C/h during a period of up to four days before the crucible was quenched to room temperature. This resulted in single crystalline black hexagonal platelets of up to 6 mm^3 in volume. Larger CuCrO_2 crystals (up to 60 mm^3) were grown with a flux melting technique based on Bi_2O_3 solvent at a temperature between 940°C and 1250°C , under conditions of repeating abrupt rise of temperature of $10\text{-}15^\circ\text{C}$ with subsequent cooling of $0.5\text{-}1.5^\circ\text{C/h}$.

The trigonal crystal structure (space group $R\bar{3}m$) with room temperature lattice parameters $a = 2.976 \text{ \AA}$ and $c = 17.110 \text{ \AA}$ [14] was confirmed by X-ray powder analysis of crushed crystals. Further characterization with respect to their magnetic properties was done using a SQUID-magnetometer. The obtained susceptibility curves were similar to data published previously [2, 3, 11, 12]. Identifying the same characteristic points in the susceptibility data as Kimura *et al* [2] the same two characteristic phase transition temperatures, $T_{N1} = 24.2 \text{ K}$ and $T_{N2} = 23.6 \text{ K}$, were obtained for our samples.

Neutron single crystal diffraction experiments were performed on the TriCS four circle diffractometer at the SINQ facility, PSI, Switzerland, on the HB-1 triple axis spectrometer and the HB-3A four circle diffractometer (FCD) at HFIR at Oak Ridge National Laboratory (ORNL), and on the Cold Neutron Chopper Spectrometer (CNCS) at the Spallation Neutron Source (SNS) in Oak Ridge. The TriCS experiment used

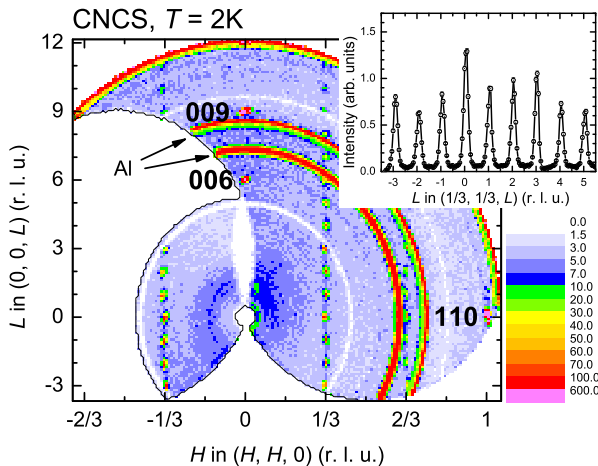


Figure 1. (colour online) Reciprocal HHL map of CuCrO_2 measured on CNCS at $T = 2 \text{ K}$. The nuclear (110) , (006) and (009) Bragg peaks as well as the polycrystalline rings from the Al sample mount are marked. The unmarked reflections are magnetic. The inset in the upper right corner shows a section along $(1/3, 1/3, L)$.

a single crystal of dimensions $3.5 \text{ mm} \times 3 \text{ mm} \times 1 \text{ mm}$ mounted in two different orientations: with the $[00L]$ direction (hexagonal setting) along the ϕ -shaft of the instrument (orientation 1) and with the $[\overline{H}H0]$ direction (orientation 2) along the ϕ -shaft. Orientation 1 gives good resolution in the H, K planes ($L=\text{const}$), while orientation 2 yields good resolution in the planes orthogonal to $[\overline{H}H0]$. For data collection in a broad \mathbf{Q} range a neutron wavelength of $\lambda = 1.178 \text{ \AA}$ (Ge-311 monochromator with vertical focusing [15]) was used without collimation between the sample and the ^3He single tube detector. For collecting maps and scans with high resolution a neutron wavelength of 2.32 \AA was used (PG-002 monochromator, PG filter) with a $20'$ collimation in front of the detector. The experiments on HB-3A FCD at HFIR used a single crystal of similar size, $3.2 \text{ mm} \times 2.5 \text{ mm} \times 1.0 \text{ mm}$, from the same batch. The crystal was mounted in the orientation 2. The neutron wavelength was $\lambda = 1.536 \text{ \AA}$ (Si-220 monochromator in high resolution mode (bending 150) [16]) with a 8 mm pinhole mask in front of the detector. Maps collected on the TriCS diffractometer used a 40 step grid with a stepsize of 0.001 reciprocal lattice units (r.l. u.). On HB-3A a 30 step grid with 0.002 r. l. u. step size was used. In order to avoid confusion, the HK -values of the scans have been transformed to an orthogonal system using the HH direction as x and the $\overline{H}H$ direction as y . Additional data were taken with elastic measurements on the HB-1 spectrometer at HFIR and on CNCS at the SNS [17]. These experiments were performed with the intent to measure the magnetic excitation spectrum and therefore the sample consisted of 10 co-aligned single crystals in (HHL) scattering geometry mounted on an aluminium sheet. On HB-1 the neutron wavelength of 2.46 \AA from a PG-002 monochromator was used. The collimation was $48'-60'-60'-240'$ with additional PG filters in the incident beam. The incident wavelength at CNCS was 2.60 \AA .

Two data sets of nuclear Bragg reflections (40 and 65 reflections for the orientations 1 and 2, respectively) were collected on TriCS for a scale factor determination at 300 K and at 5 K with $\lambda = 1.178 \text{ \AA}$. These measurements proved the absence of reverse/obverse twinning [18] and confirmed the published nuclear structure [14].

3. Results

A diffraction map measured at $T = 2 \text{ K}$ on CNCS is shown in figure 1. With this pattern it is clear that the magnetic order is truly 3-dimensional, in fact all measurements find the full width at half maximum (FWHM) in the L -direction to be resolution limited (insert in 1). The correlation length is therefore larger than at least several hundred \AA . This result clearly disagrees with the conclusions from the powder diffraction measurements [10, 11] (which were suggesting short range order along the L -direction).

To identify the fundamental magnetic propagation vector, a detailed mapping of the magnetic reflections in the basal plane(s) has been performed at $T = 5 \text{ K}$ for both the TriCS and HB-3A datasets. Figure 2 gives an overview over the measured magnetic reflections and the related nuclear reflections to which they are satellite. The results are shown for the magnetic reflections with $L = 0, 1, 2$ around $(1/3, 1/3, L)$

and around $(-1/3, 2/3, L)$ in figure 3. The figure shows the projection of the three observed reflections in the H, K -plane. The magnetic reflections are located around the commensurate $1/3$ position which is also shown.

Based on our measurements, the magnetic structure of CuCrO_2 can be satisfactorily described with a pair of incommensurate propagation vectors $(\boldsymbol{\tau}_1, -\boldsymbol{\tau}_1)$ with $\boldsymbol{\tau}_1 = (\tau, \tau, 0)$ and $\tau = 0.3298(1)$. By symmetry, the star of the propagation vector consists of $\boldsymbol{\tau}_1 = (\tau, \tau, 0)$, $\boldsymbol{\tau}_2 = (\tau, -2\tau, 0)$ and $\boldsymbol{\tau}_3 = (-2\tau, \tau, 0)$.

To confirm the magnetic structure a refinement of the two datasets measured at TriCS, collected with $\lambda=1.178 \text{ \AA}$ (140 reflections) and $\lambda=2.32 \text{ \AA}$ (197 reflections) has been performed using FullProf [19]. Three magnetic domains due to the 3-fold axis have been taken into account. The following four models for the arrangement of magnetic moments were considered:

- amplitude modulated structure derived from the “Proper Helix”
- “Cycloid 1” with moments rotating in the $[110]$ - $[001]$ -plane
- “Cycloid 2” with moments rotating in the $[110]$ - $[1\bar{1}0]$ -plane
- the “Proper Helix” with moments rotating in the $[1\bar{1}0]$ - $[001]$ -plane as in [12]

The possibility of an elliptical envelope was allowed for the three last cases. Generally the magnetic moment \mathbf{M} of the Cr^{3+} ion in the l th unit cell can be described by the generalized helix presentation,

$$\mathbf{M}_l = \mathbf{M}_1 \cos(\boldsymbol{\tau} \cdot \mathbf{r}_l + \psi) + \mathbf{M}_2 \sin(\boldsymbol{\tau} \cdot \mathbf{r}_l + \psi) ,$$

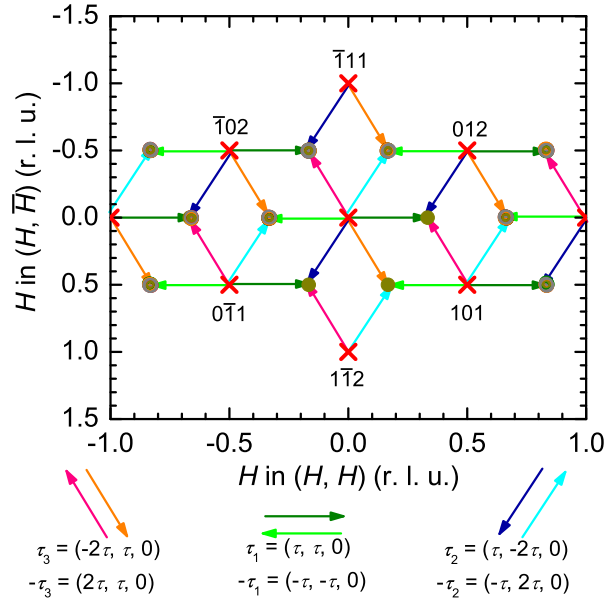


Figure 2. (Colour online) HK -projection of the magnetic reflections (circles) and their origin. The crosses mark the position of the nuclear reflections. The star of the propagation vector τ is indicated by the different coloured arrows.

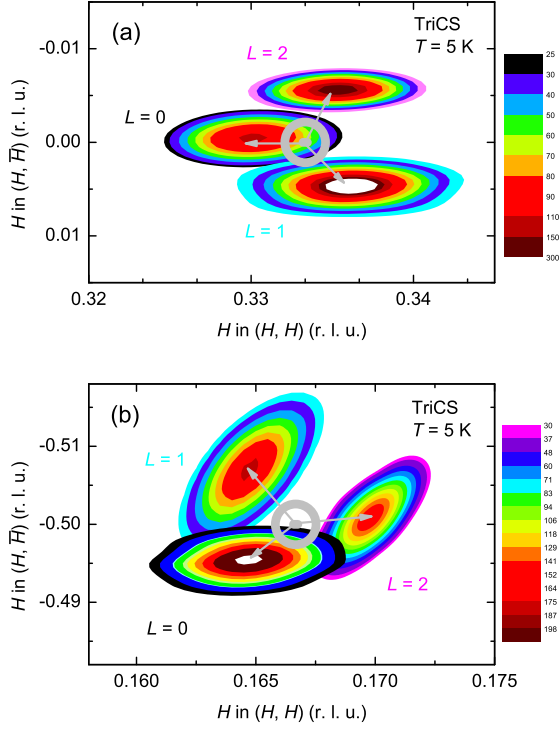


Figure 3. (Colour online) Upper panel: H, K -projection of the magnetic reflections around the $(1/3, 1/3, L)$ position (grey point) as measured on TriCS. Lower panel: magnetic reflections around the $(-1/3, 2/3, L)$ position

where \mathbf{M}_1 and \mathbf{M}_2 are orthogonal base vectors determining the magnitude and direction of the generalized helix and ψ is the phase.

The results for our refinement are listed in table 1. The cycloid models fit the experimental data poorly since they predict small intensities for the magnetic satellites along the wavevectors (i.e τ_1, τ_2, τ_3).

Table 1. Reliability factors for the magnetic structure at $T = 5$ K measured with $\lambda=1.178$ Å . Four different proto-type magnetic structures have been considered: Amplitude modulated, Cycloid 1 (ab -cycloid), Cycloid 2 (110- c -cycloid) and Proper helix. The refined parameters were the magnetic moment and the domain population.

Refined set of 140 magnetic reflections measured with 1.178Å				
	Ampl. Mod.	Cycloid 1	Cycloid 2	Proper helix
RF ²	35.0	43.1	35.1	28.0
RF ² w	38.1	44.7	38.1	30.6
RF	20.8	24.0	20.8	13.7
$M_1(\mu_B)$	$[1\bar{1}0] -0.1(6)$	$[110] 1(1)$	$[110] 0(8)$	$[1\bar{1}0] 2.2(2)$
$M_2(\mu_B)$	$[001] 3.3(2)$	$[1\bar{1}0] 3.2(4)$	$[001] 3.4(4)$	$[001] 2.8(2)$
Domain population (%)	39(7) : 36(6) : 25(7)	39(9) : 40(9) : 22(9)	39(8) : 36(8) : 25(9)	37(2) : 37(2) : 26(3)

In reality these intensities are large. This indicates that the magnetic moment is predominantly orthogonal to the wavevector. The amplitude modulated model agrees

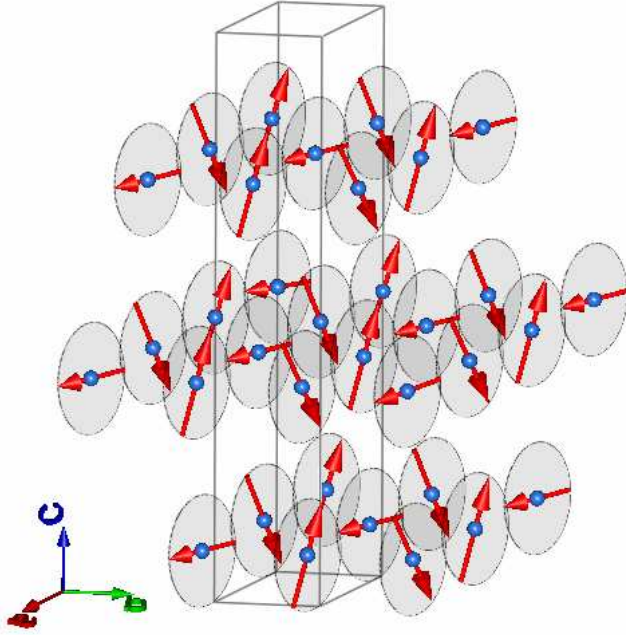


Figure 4. (Colour online) Real space representation of the magnetic structure of CuCrO_2 . The chemical unit cell is outlined.

slightly better with the data, but the agreement factors are larger than the ones obtained with the “Proper Helix” model. Therefore, we agree with the powder diffraction results of Poienar *et al* [11] and polarized data of Soda *et al* [12] that the magnetic structure in CuCrO_2 is a proper helix. The statistically best fit is obtained for an elliptical helix with the moments averaged over all domains $\mathbf{M}_{[\bar{1}\bar{1}0]} = 2.2(2) \mu_B$ and $\mathbf{M}_{[001]} = 2.8(2) \mu_B$. The data yields a different population for each domain. For the helix the obtained population is 37(2)% : 37(2)% : 26(3)% . In principle $\boldsymbol{\tau}_1$ and $-\boldsymbol{\tau}_1$ are not equivalent wave vectors and they might correspond to two different structures. Such situation is however energetically not favored and we considered $\boldsymbol{\tau}_1$ and $-\boldsymbol{\tau}_1$ as generators to two chiral domains of the same structure. Figure 4 depicts the real space representation of the “Proper Helix” model.

We next discuss the temperature dependence of the magnetic structure. The magnetic intensity as shown in figure 5 decreases strongly with temperature above ~ 23 K and would be in agreement with a critical temperature slightly below 24 K. However, the magnetic intensity above 24 K is still significant. Therefore the half-widths of the magnetic reflections were also analyzed along different lattice directions. Figure 6 shows three measurements for both the H, H and the L direction, below T_{N2} , between T_{N1} and T_{N2} , and above T_{N1} , respectively. Measured along the H, H -direction the magnetic Bragg peak loses roughly a factor of four in intensity between 22 K and 24 K but the width changes only slightly. At 26 K the magnetic intensity is then close to the background and the intensity broadly smeared as expected above (but close to) the magnetic ordering temperature. Apparently T_{N2} is not a critical temperature along this

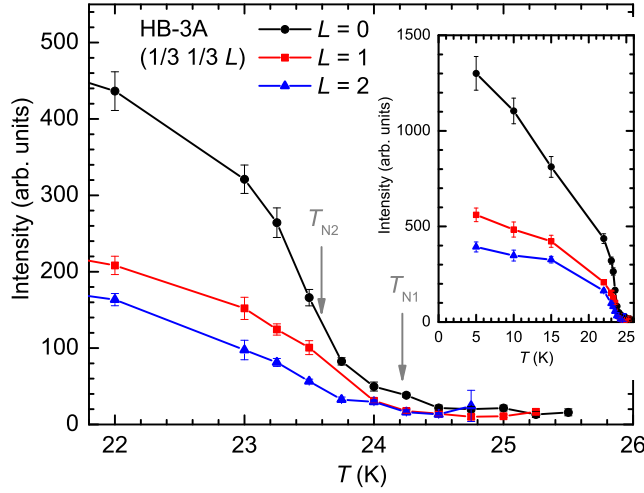


Figure 5. (Colour online) Intensity vs. temperature plot for the magnetic reflections around $(1/3, 1/3, L)$ in the region from 22 to 26 K from measurements on HB-3A. The two transition temperatures T_{N1} and T_{N2} are marked. The entire temperature range is shown as inset.

direction. In the lower panel of figure 6 measurements along the L -direction at the same temperatures are shown for comparison. Here, no sign of a Bragg peak can be seen in the intermediate temperature range, whereas along H , H there is still a peak, albeit small, at the same temperature. Along the L -direction one finds *diffuse* magnetic scattering between T_{N1} and T_{N2} , well above instrument background, indicative of a complete loss of the magnetic near neighbor correlations along this direction. Since the measurement uses energy analysis, the magnetic correlations can be considered static.

The picture becomes clear with an analysis of the temperature dependence of the widths of the Bragg peaks. This is shown in figure 7. The trend for the peak width along the HH direction is shown in the upper panel of figure 7. The width increases at increasing temperatures starting around 24 K. Above 25 K it then becomes difficult to fit a peak to the data. In contrast, the width along the L -direction as shown in the lower panel of the figure start to significantly increase already above 23.6 K. At 24 K the fitted width is already as large as the distance between reciprocal lattice points.

To summarize, the picture that emerges is that CuCrO_2 enters a truly 2-dimensional ordered state between T_{N1} and T_{N2} , with well developed long range correlations in the H, K plane but a lack of correlation in the L -direction. Only below T_{N2} a 3-dimensional ordering is established.

4. Discussion

The new single crystal diffraction data and our analysis show that the low temperature magnetic ordering of CuCrO_2 is fully 3-dimensional and can be described as a incommensurate proper helix propagating in the $[H, H, 0]$ direction. Moments are in the $[H, \bar{H}, L]$ plane. The envelope of the spiral is slightly elliptic. The magnetic propagation

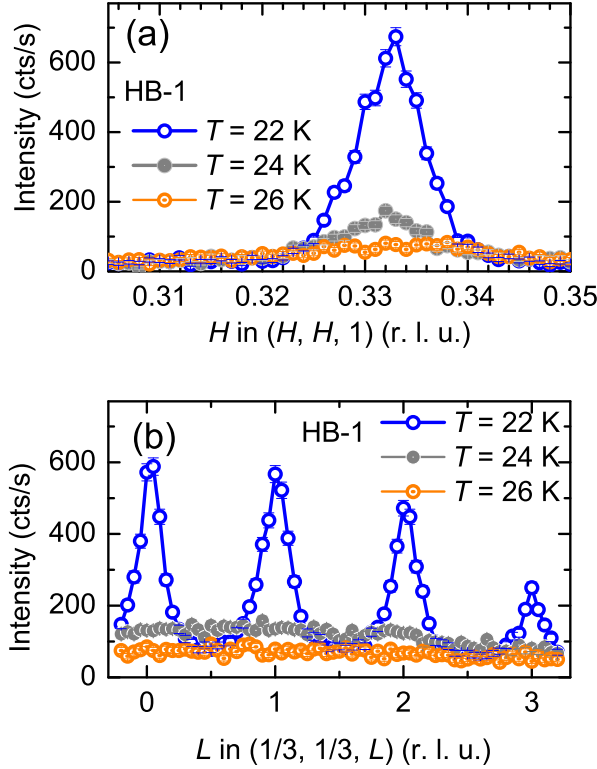


Figure 6. (Colour online) Magnetic intensities at three temperatures measured along the HH direction (a) and along the L direction (b) on HB-1.

vector τ is very close to the commensurate $(1/3, 1/3, 0)$ value. The commensurate case would correspond to the classic 120° magnetic ground state of the 2-dimensional triangular lattice. The cause of the incommensurability of the propagation vector has been discussed earlier, and two different explanations have been proposed: either an in-plane lattice distortion [4, 5] or interlayer exchange interaction [20–23]. The latter is in better agreement with the occurrence of 3-dimensional order, although it had been shown that an interlayer exchange has to be relatively small ($<0.2\text{meV}$) [24]. The maximum ordered moment in our model is $2.8(2) \mu_B$ which is close to the expected $3 \mu_B$ for the Cr^{3+} ion and the reported values from the powder measurements [10, 11]. An additional uncertainty for the absolute moment value from the single crystal measurements comes from the non-equal domain distribution. A cycloidal spin structure can be excluded from our analysis, in accordance with the observation of multiferroicity in the low temperature phase and its explanation after Arima [6, 12, 25]. The 3D character of the low temperature ordering is in agreement with the interpretation of the earlier published specific heat data at the phase transition [11].

The multiferroic state of CuCrO_2 is entered without an apparent structural symmetry reduction or lattice distortion. Within the resolution of our experiments the upper limit for change of the lattice constants at the phase transition is 0.001 \AA . However,

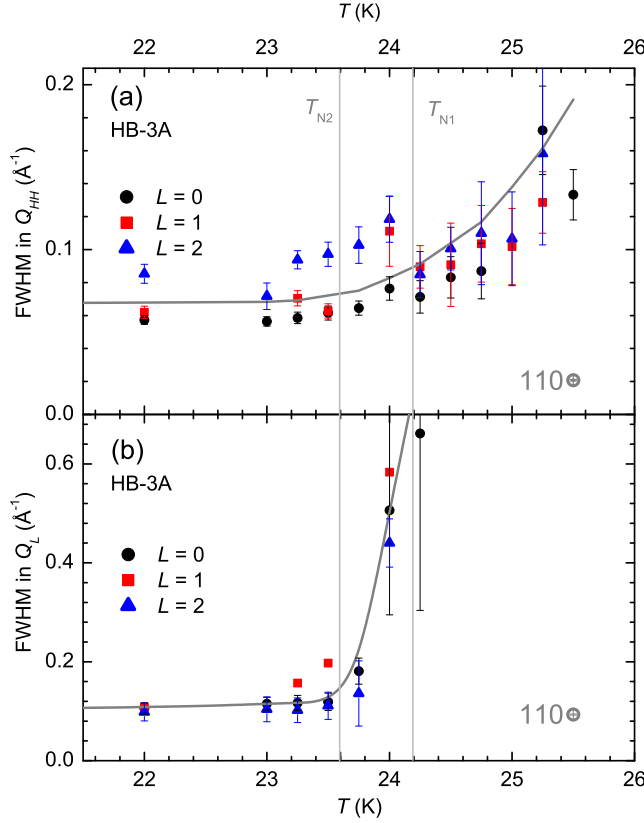


Figure 7. (Colour online) Temperature dependence of the FWHM of the magnetic satellites measured on HB-3A along (a) the HH direction and (b) along the L direction in the temperature range from 22 K to 26 K. The lines are guides to the eye. The gray points at 25.5 K are the measured FWHM of the nuclear 110 reflection at room temperature. The vertical gray lines mark the transition temperatures T_{N1} and T_{N2} . The width of the Bragg peaks along L diverges approx. 1 K below the temperature at which it diverges along HH .

evidence for in-plane distortions have been observed in high resolution X-ray diffraction measurements [5]. This is in agreement with small structural distortion observed in the related CuFeO_2 system [9].

Why is CuCrO_2 not multiferroic between T_{N1} and T_{N2} ? According to the Arima model [25] the in-plane proper screw spiral will create a spontaneous polarization even without the observed 3-dimensional order. The propagation vector in the narrow phase is the same as in the multiferroic phase and it will be argued in the following why the magnetic structure in the intermediate phase is most likely an in-plane proper screw but without interlayer order. In the light of the 2-dimensional nature this narrow phase has been discussed as a possible collinear state [2]. However, it is unlikely that the narrow temperature phase has a collinear structure. It has been shown theoretically [26] that the collinear state is energetically not favored. Also, a collinear state with three sublattices would have a net ferromagnetic moment (which is not observed). A re-ordering from collinear to helical state is expected to feature a large response in the temperature

dependent susceptibility (which is not observed). Similar, an amplitude modulated magnetic structure on a three sub lattice without a ferromagnetic net moment would undergo a discontinues phase transition to a spiral state.

The same propagation vector in both phases with the absence of a net ferromagnetic component and the continuous course of the susceptibility through the transition at T_{N2} indicate that spirals already form at T_{N1} . The uncorrelated spirals then order through ferromagnetic interlayer exchange to a full 3-dimensional order at T_{N2} . The question why CuCrO₂ is not multiferroic between T_{N1} and T_{N2} cannot be answered with the results from the diffraction experiment alone since in the picture of the uncorrelated spirals the spontaneous polarization could be averaged to zero. A possible experiment to clarify this question is neutron diffraction with an applied electric field in this narrow phase.

Acknowledgments

We acknowledge the technical and scientific support from the staff at SNS, HFIR, and PSI. This work was partly performed at SINQ, Paul Scherrer Institute, Villigen, Switzerland. This research was sponsored by the Division of Materials Sciences and Engineering of the U. S. Department of Energy. Research at Oak Ridge National Laboratory's Spallation Neutron Source was supported by the Scientific User Facilities Division, Office of Basic Energy Sciences, U. S. Department of Energy. The work in Minsk was supported in part by Belarusian Fund for Basic Scientific Research, grant No F10R-154.

- [1] Sang-Wook Cheong and Maxim Mostovoy. Multiferroics: a magnetic twist for ferroelectricity. *Nature Materials*, 6(1):13, January 2007.
- [2] Kenta Kimura, Hiroyuki Nakamura, Kenya Ohgushi, and Tsuyoshi Kimura. Magnetoelectric control of spin-chiral ferroelectric domains in a triangular lattice antiferromagnet. *Phys. Rev. B*, 78(14):140401(R), October 2008.
- [3] K. Kimura, H. Nakamura, S. Kimura, M. Hagiwara, and T. Kimura. Tuning ferroelectric polarization reversal by electric and magnetic fields in CuCrO_2 . *Phys. Rev. Lett.*, 103(10):107201, September 2009.
- [4] H. Yamaguchi, S. Ohtomo, S. Kimura, M. Hagiwara, K. Kimura, T. Kimura, T. Okuda, and K. Kindo. Spiral-plane flop probed by esr in the multiferroic triangular-lattice antiferromagnet CuCrO_2 . *Phys. Rev. B*, 81(3):033104, January 2010.
- [5] Kenta Kimura, Tsuyoshi Otani, Hiroyuki Nakamura, Yusuke Wakabayashi, and Tsuyoshi Kimura. Lattice distortion coupled with magnetic ordering in a triangular lattice antiferromagnet CuCrO_2 . *Journal of the Physical Society of Japan*, 78(11):113710, 2009.
- [6] Minoru Soda, Kenta Kimura, Tsuyoshi Kimura, Masato Matsuura, and Kazuma Hirota. Electric control of spin helicity in multiferroic triangular lattice antiferromagnet CuCrO_2 with proper-screw order. *Journal of the Physical Society of Japan*, 78(12):124703, 2009.
- [7] O. A. Petrenko, G. Balakrishnan, M. R. Lees, D. McK. Paul, and A. Hoser. High-magnetic-field behavior of the triangular-lattice antiferromagnet CuFeO_2 . *Phys. Rev. B*, 62(13):8983, February 2000.
- [8] T. Kimura, J. C. Lashley, and A. P. Ramirez. Inversion-symmetry breaking in the noncollinear magnetic phase of the triangular-lattice antiferromagnet CuFeO_2 . *Phys. Rev. B*, 73(22):220401(R), June 2006.
- [9] F. Ye, Y. Ren, Q. Huang, J. A. Fernandez-Baca, Pengcheng Dai, J. W. Lynn, and T. Kimura. Spontaneous spin-lattice coupling in the geometrically frustrated triangular lattice antiferromagnet CuFeO_2 . *Phys. Rev. B*, 73(22):220404(R), June 2006.
- [10] H Kadowaki, H Kikuchi, and Y Ajiro. Neutron powder diffraction study of the two-dimensional triangular lattice antiferromagnet CuCrO_2 . *Journal of Physics: Condensed Matter*, 2(19):4485, 1990.
- [11] Maria Poienar, Françoise Damay, Christine Martin, Vincent Hardy, Antoine Maignan, and Gilles André. Structural and magnetic properties of CuCr_2S_2 by neutron powder diffraction. *Phys. Rev. B*, 79(1):014412, January 2009.
- [12] Minoru Soda, Kenta Kimura, Tsuyoshi Kimura, and Kazuma Hirota. Domain rearrangement and spin-spiral-plane flop as sources of magnetoelectric effects in delafossite CuCrO_2 . *Phys. Rev. B*, 81(10):100406(R), March 2010.
- [13] O. Crottaz, F. Kubel, and H. Schmid. Preparation of trigonal and hexagonal cuprous chromite and phase transition study based on single crystal structure data. *Journal of Solid State Chemistry*, 122(1):247 – 250, 1996.
- [14] O. Crottaz and F. Kubel. Crystal structure of copper(i) chromium(iii) oxide, 3r-CuCrO_2 . *Zeitschrift für Kristallographie*, 211(7):482 – 482, 1996.
- [15] J. Schefer, M. Könnicke, A. Murasik, A. Czopnik, Th. Strässle, P. Keller, and N. Schlumpf. Single-crystal diffraction instrument trics at sinq. *Physica B: Condensed Matter*, 276-278:168 – 169, 2000.
- [16] Bryan C. Chakoumakos, Huibo Cao, Feng Ye, Alexandru D. Stoica, Mihai Popovici, Madhan Sundaram, Wenduo Zhou, J. Steve Hicks, Gary W. Lynn, and Richard A. Riedel. Four-circle single-crystal neutron diffractometer at the High Flux Isotope Reactor. *Journal of Applied Crystallography*, 44(3):655–658, Jun 2011.
- [17] T. E. Mason, D. Abernathy, I. Anderson, J. Ankner, T. Egami, G. Ehlers, A. Ekkebus, G. Granroth, M. Hagen, K. Herwig, J. Hodges, C. Hoffmann, C. Horak, L. Horton, F. Klose, J. Larese, A. Mesecar, D. Myles, J. Neufeld, M. Ohl, C. Tulk, X. L. Wang, and J. Zhao. The spallation neutron source in oak ridge: A powerful tool for materials research. *Phys. B*

- (Amsterdam, Neth.), 385-386(Pt. 2):955–960, 2006.
- [18] R. Herbst-Irmer and G. M. Sheldrick. Refinement of obverse/reverse twins. *Acta Crystallographica Section B*, 58(2):477–481, jun 2002.
 - [19] Juan Rodríguez-Carvajal. Recent advances in magnetic structure determination by neutron powder diffraction. *Physica B: Condensed Matter*, 192(1-2):55 – 69, 1993.
 - [20] E Rastelli and A Tassi. The rhombohedral heisenberg antiferromagnet: infinite degeneracy of the ground state and magnetic properties of solid oxygen. *Journal of Physics C: Solid State Physics*, 19(19):L423, 1986.
 - [21] E Rastelli and A Tassi. Order produced by quantum disorder in the heisenberg rhombohedral antiferromagnet. *Journal of Physics C: Solid State Physics*, 20(15):L303, 1987.
 - [22] E Rastelli and A Tassi. Collinear and helical phases of the monoclinic and rhombohedral antiferromagnet. application to the - and -phases of solid oxygen. *Journal of Physics C: Solid State Physics*, 21(5):1003, 1988.
 - [23] H Kadowaki, H Takei, and K Motoya. Double-q 120 degrees structure in the heisenberg antiferromagnet on rhombohedrally stacked triangular lattice licro 2. *Journal of Physics: Condensed Matter*, 7(34):6869, 1995.
 - [24] M. Poienar, F. Damay, C. Martin, J. Robert, and S. Petit. Spin dynamics in the geometrically frustrated multiferroic cucro2. *Phys. Rev. B*, 81(10):104411, March 2010.
 - [25] T. Arima. Ferroelectricity induced by proper-screw type magnetic order. *Journal of the Physical Society of Japan*, 76(7):073702, July 2007.
 - [26] Randy S. Fishman. Phase diagram of a geometrically frustrated triangular-lattice antiferromagnet in a magnetic field. *Phys. Rev. Lett.*, 106(3):037206, Jan 2011.